Multiuser MIMO in Distributed Antenna Systems With Out-of-Cell Interference

Robert W. Heath, Jr., *Fellow, IEEE*, Tao Wu, Young Hoon Kwon, and Anthony C. K. Soong, *Senior Member, IEEE*

***Abstract*—Distributed antenna systems (DAS) augment the base station's transmit capability by adding multiple remote radio units, connected to the base station via a high bandwidth and low latency link. With DAS, the base station operates as if it had multiple antennas, but the antennas happen to be in different geographic locations. DAS have been shown to enhance coverage and capacity in cellular systems, in a variety of different configurations. This paper proposes, analyzes, and compares several downlink multiuser multiple input multiple output (MIMO) DAS strategies in terms of per-user throughput and area spectral efficiency. Zero-forcing transmit beamforming is used for transmission, the remote radio units may have one or more antennas, and the subscriber has a single receive antenna. Techniques considered include beamforming across all remote radio units (full transmission), using the same beamforming vector for each remote radio unit (simplified transmission), and selecting a subset of remote radio units. To facilitate rapid simulation and design space exploration, approximations of the ergodic rate are proposed for each technique assuming path-loss, small-scale Rayleigh fading, and out-of-cell interference. Simulations accounting for multiple interfering cells are used to compare the different transmission techniques. Full transmission is found to have the best performance even accounting for out-of-cell interference, though gains diminish for higher numbers of active users. Simplified transmission improves over no DAS but performance degrades with more active remote radio units.**

***Index Terms*—Cellular networks, 4-G mobile communication, multiple-input–multiple-output (MIMO).**

I. Introduction

CELLULAR systems can make use of remote radio units to provide more uniform coverage especially in shadowed and indoor locations. The remote radio units may have one or more antennas and are connected to a home base station (or central processing unit) using a high-bandwidth low-latency dedicated connection, creating what are widely known as distributed antenna systems (DAS) [1], [2]. In DAS, the remote radio units (RRUs) have minimal intelligence of their own; essentially they are an extension of the base station antenna ports. Previous work with single antenna RRUs has established the benefits of DAS for improving indoor coverage [3], [4], reducing outage on the downlink [5], [6], reducing outage on the uplink [7], and increasing capacity [8]. DAS works with different multiple access technologies [9]–[11]. Unlike cellular systems with fixed relays [12], [13], DAS does not incur an over-the-air penalty for transmissions to and from the RRU. Compared with a femtocell architecture [14], the RRUs are fully coordinated by the central processing unit and are not likely to be installed by the subscriber.

As interest in multiple input multiple output (MIMO) communication has grown, DAS has embraced multiple antennas at the RRU for more sophisticated downlink transmission. One focus has been on distributed spatial multiplexing. Neglecting out-of-cell interference, prior work has shown that fully distributed antennas (one antenna at each RRU) yield higher sum rates than having antennas co-located at the base station or having multiple antennas at each RRU [15]–[18] for the same number of antennas thanks to macrodiversity gain. In simulations with interference, [19] finds that in the presence of significant interference, co-locating some antennas at each RRU can improve throughput due to the small-scale diversity gain. When RRUs serve different users and interfere with each other, [20] finds that having about as many antennas per RRU as on the subscriber is optimum. Another focus of prior work has been on transmit diversity across the distributed antennas for single antenna subscribers. Accounting for out-of-cell interference, [8] shows that the best transmit beamforming strategy is selecting the best antenna; the gain from co-phasing multiple transmit antennas does not compensate for the excess interference created from other cells. The results also hold using randomly located RRUs [21]. Limited feedback beamforming [22] has also been considered in DAS for transmission across the antenna elements [23], as well as beamforming at the array on each RRU [24], but these results did not consider the impact of interference.

Another application of multiple antennas is multiuser MIMO communication, where simultaneous transmission to (on the downlink) or reception from (on the uplink) multiple users increases the sum rate [25]. The application of multiuser MIMO to DAS has received less attention. Most work focuses on the uplink. In [26], DAS is shown to decrease the required uplink transmit power and to increase the sum capacity versus having centralized antennas. In [27], subscribers communicate with one or more RRUs, but collaborative processing is not used to decode all the users; interference from other users is treated as noise therefore the full benefits of multiuser MIMO are not achieved. On the downlink, [28] designs multiuser transmit beamformers for centralized systems and DAS by maximizing a link adaptation function. For a particular DAS configuration

Manuscript received February 04, 2011; revised June 10, 2011; accepted June 14, 2011. Date of publication July 14, 2011; date of current version September 14, 2011. The associate editor coordinating the review of this manuscript and approving it for publication was Dr. Ta-Sung Lee. The material in this paper was presented at the Asilomar Conference on Signals, Systems, and Computers2010

R. W. Heath Jr. is with MIMO Wireless, Inc.. He is also with The University of Texas at Austin, Austin, TX 78712 USA (e-mail: rheath@mimowireless.com).

T. Wu is with Broadcom Corporation, Sunnyvale, CA 92617 USA (e-mail: tawu@broadcom.com).

Y. Kwon is with Huawei Technologies, San Diego, CA 92121 USA (e-mail: ykwon@huawei.com).

A. C. K. Soong is with Huawei Technologies, Plano, TX 75075 USA (e-mail: asoong@huawei.com).

Color versions of one or more of the figures in this paper are available online at http://ieeexplore.ieee.org.

Digital Object Identifier 10.1109/TSP.2011.2161985

with sectored antennas, they show that beamforming in DAS provides stronger and more stable coverage than the centralized approach, though out-of-cell interference is neglected. Simulation results in [29] for several different transmission techniques, incorporating realistic channel parameters and interference, show that orthogonal transmission between RRUs is preferred in some cases, though full multiuser MIMO was not considered. Results in [30] show that multiuser MIMO DAS outperforms selecting the best user in the presence of out-of-cell interference. While the results in [30] consider scheduling, only three single antenna RRUs are considered and expressions for ergodic rates are not provided. Multicell MIMO (also known as network MIMO or base station cooperation), can be viewed as a DAS where each base station becomes a RRU and a cluster of base stations acts as a DAS [31]. There are some important differences though. In multicell MIMO where multiple base stations are coordinated through the cellular backhaul, the bandwidth of the backhaul link and delay create additional impairments [32], [33]. Because DAS employs dedicated connections to the RRU, e.g., using radio over fiber [34], bandwidth and delay are not a significant concerns in DAS. Some prior work on multicell MIMO deals with interference through multiple levels of coordination [35]. DAS deployments may have little coordination between base stations; therefore interference can not be neglected when evaluating DAS performance.

Establishing multiuser MIMO as a viable transmission strategy in DAS requires explicitly accounting for the effects of interference. The presence of interference can change the preferred operating conditions in MIMO systems. In multiuser MIMO, depending on the channel state information available, the optimum number of users selected for transmission and the number of streams varies as functions of the signal-to-interference-plus-noise ratio (SINR) [36]. In single user DAS, antenna selection is preferred over beamforming in terms of ergodic rate when out-of-cell interference is incorporated into the model [8]. Based on prior work, it is not clear if a multiuser MIMO in DAS should use all possible distributed antennas or a subset of antennas. Further it is unclear how many users should be active, on average, to make the right tradeoff between coverage and capacity.

In this paper, we show that multiuser MIMO is an effective strategy for DAS even in the presence of out-of-cell interference. We consider a narrowband DAS channel model with independent Gaussian distributed small-scale fading and distance-dependent path-loss. Since we will compute ergodic rates as a function of distance and area spectral efficiency [37], which averages throughput over the cell, we neglect the large-scale fading component. The RRUs may have one or more transmit antennas while the subscriber has a single receive antenna. Extending the results to multiple receive antennas using transmit strategies like [38] is an interesting topic of future work. We propose several multiuser downlink transmission strategies for DAS based on zero-forcing beamforming. With *full transmission*, multiuser MIMO is applied across the entire distributed array. With *simplified transmission*, each RRU uses the same set of beamforming vectors. This is essentially a multiuser version of the blanket transmission in [8]. We compare full and simplified transmission for multiuser MIMO DAS with a simplified large-scale selection algorithm that depends only on the path loss in the home cell, not the instantaneous channel coefficients or the interference channel. Compared with our prior work in [39] this paper provides more results on Gamma random variables, including the exact distribution of the sum of Gamma random variables, as well as more justification of the high SNR (signal-to-noise ratio) approximation, the moment matching approximation, and the truncated exact solution. It also includes the simplified transmission approach and discusses an algorithm for RRU selection.

To facilitate rapid simulation and design space exploration, we propose approximations of the ergodic rate (averaging over the small scale fading) for each technique assuming path-loss, small-scale Rayleigh fading, and out-of-cell interference. The general mathematical approach is to leverage properties of Gamma distributed random variables, especially the simple form of the expectation of the log of a Gamma random variable. We use closed form expressions of sums of Gamma random variables [40]–[43]) to propose several expressions for calculating the sum rates in the presence of co-channel interference. We describe a particularly simple approach using moment matching to approximate the sum of Gamma random variables with another Gamma random variable. We also leverage some results from [36] on multiuser MIMO in the presence of interference, and exploit some properties of isotropic distributions. For a given configuration, our mathematical expressions provide expected rate as a function of location, which can be subsequently averaged in the cell to compute outage or area spectral efficiency. They reduce system simulation time and facilitate studying different system parameters, e.g., the number of active users, the number of RRUs, or the number of antennas per RRU.

We simulate several multiuser MIMO DAS strategies and make several important observations: (i) full transmission across all RRUs offers throughputs that increase with the number of RRUs and the number of antennas per RRU; (ii) the simplified transmission approach still improves over the non-DAS multiuser MIMO, though full transmission performs much better; (iii) peaks in the area spectral efficiency are observed when about half the maximum number of possible users is active; and (iv) if the optimum number of users is allowed to scale, the area spectral efficiency increases as the number of RRUs increases. Thus multiuser MIMO is a viable transmission strategy for DAS even in the presence of interference.

Organization: This paper is organized as follows. In Section II, we review some known results that will be used to develop ergodic rate approximations in the presence of interference. Then in Section III we introduce the narrowband MIMO downlink DAS channel model under consideration. In Sections IV–VI we introduce different multiuser MIMO DAS strategies including the baseline case (no DAS), full transmission (sending different signals from all antennas), and simplified transmission (sending the same signal from each RRU). We present approximations of the ergodic rate for each strategy. In Section VII, we compare the different strategies in different configurations as a function of the number of users, number of antennas, and number of RRUs. We also evaluate the impact of a simple RRU selection algorithm. Finally in Section VIII we draw some conclusions and point out some topics of future work.

Notation: We use the following notation throughout this paper: bold lowercase $\mathbf{a}$ is used to denote column vectors, bold uppercase $\mathbf{A}$ is used to denote matrices, nonbold letters a, A are used to denote scalar values, and caligraphic letters $\mathcal{A}$ to denote sets. Using this notation, $|a|$ is the magnitude of a scalar, $|\mathbf{A}|$ is

the determinant, $\|\mathbf{a}\|$ is the L-2 norm, $\|\mathbf{A}\|_F$ is the Frobenius norm, $\lambda_k(\mathbf{A})$ denotes the k^{th} eigen value of $\mathbf{A}$ in decreasing order, $\sigma_k(\mathbf{A})$ denotes the k^{th} singular value of $\mathbf{A}$ in decreasing order, $\mathrm{tr}(\mathbf{A})$ denotes the trace, $\mathbf{A}^*$ is the conjugate transpose, $\mathbf{A}^T$ is the matrix transpose, $\mathbf{A}^{-1}$ denotes the inverse of a square matrix, $\mathbf{A}^\dagger$ is the Moore-Penrose pseudo inverse, $\mathbf{a}_k$ is the k^{th} entry of vector $\mathbf{a}$, $[\mathbf{A}]_{k,l}$ is the scalar entry of $\mathbf{A}$ in k^{th} row l^{th} column, $[\mathbf{A}]_{:,k}$ is the k^{th} column of matrix $\mathbf{A}$, $[\mathbf{A}]_{:,k:m}$ is the column consisting of rows $k, k+1, \ldots, m$ of matrix $\mathbf{A}$, $[\mathbf{a}]_k$ is the k^{th} entry of $\mathbf{a}$, $|\mathcal{A}|$ is the cardinality of set $\mathcal{A}$, and $:=$ denotes definition. We use the notation $\mathcal{N}(\mathbf{m}, \mathbf{R})$ to denote a complex circularly symmetric Gaussian random vector with mean $\mathbf{m}$ and covariance $\mathbf{R}$. We use $\mathbb{E}$ to denote expectation.

II. Mathematical Preliminaries

In this paper we compute ergodic rates, where the average is taken with respect to the small-scale fading distribution. The calculations are based on a small-scale "Rayleigh" assumption on the channel for which it is known that the magnitude squared of the channel has the Chi-Square distribution. Because we will deal with sums of interfering signals with different path loss characteristics, we use Gamma random variables, which provide a generalization of Chi-square random variables. In this section we provide some background on Gamma random variables and summarize important results on sums of Gamma random variables. As the results are known, we omit most of the proofs. Then we propose a high SNR approximation of the ergodic mutual information using a Gamma approximation of the sum interference.

A. Gamma Random Variables

Definition 1: A Gamma random variable with finite shape $k > 0$ and finite scale $\theta > 0$, denoted as $\Gamma(k, \theta)$ has probability distribution function

$$f_X(x) = x^{k-1} \frac{e^{-x/\theta}}{\theta^k \Gamma(k)}$$

for $x \geq 0$. The mean is $k\theta$ and the variance $k\theta^2$.

Several properties of Gamma random variables are useful.

- Fact 1: If Z is a circularly symmetric complex Gaussian with $\mathcal{N}(0,1)$ (variance 1/2 per dimension) then $X = |Z|^2$ is $\Gamma(1,1)$.
- Fact 2: If X has a Chi-square distribution with $2N$ degrees of freedom then X is also $\Gamma(N, 2)$.
- Fact 3: If X is $\Gamma(k, \theta)$ then with scalar $\alpha > 0$, αX is $\Gamma(k, \alpha\theta)$.

An interesting fact about Gamma random variables is that the expectation of the log function is known, and is a simple (relatively speaking) function of the shape and gain.

Lemma 2 (Expectation of the Log): If X is a Gamma distributed random variable with parameters k and θ then

$$\mathbb{E}_X \ln X = \psi(k) + \ln(\theta) \tag{1}$$

where $\psi(k)$ is the digamma function. In terms of base two logarithms

$$\mathbb{E}_X \log_2 X = \log_2 e\, \psi(k) + \log_2(\theta). \tag{2}$$

In this paper we use Gamma distributions to compute average rates. We want to calculate functions of the form $\mathbb{E}\log(1+X)$. Lemma 2, unfortunately, only provides $\mathbb{E}\log(X)$. The exact distribution is available but has a more complex form.

Lemma 3: If X is a Gamma distributed random variable with parameters k and θ then [see (3) at the bottom of the page], where $G_{p,q}^{m,n}(\cdot)$ is the Meijer G-function and ${}_pF_q(\cdot)$ is a generalized hypergeometric function.

Proof: The results can be calculated using integral tables or, more conveniently, using a symbolic tool like Mathematica. Note that there are several ways to express the results with different generalized functions. ■

The generalized functions in Lemma 3 facilitate symbolic computations. For simulations, however, they generally require numerical integration. The expressions in Lemma 2, however, are relatively easy to compute. The digamma function is implemented in many numerical packages or its asymptotic approximation can be used $\psi(x) = \ln(x) + \frac{1}{x} + \mathcal{O}\left(\frac{1}{x^2}\right)$.

It is well known that for $x > 0$, $\log(1+x) = \log(x) + \mathcal{O}\left(\frac{1}{x}\right)$. A typical high SNR approximation is, therefore, $\log(1+x) \approx \log(x)$. Now consider $\mathbb{E}\log(1+X)$ where X is $\Gamma(k,\theta)$. First consider the noninteger case. From (3), $\mathbb{E}\log(1+X) = \mathbb{E}\log(X) + \text{other terms}$. Performing a series expansion on the other terms about $\theta \to \infty$ and looking at the zeroth coefficient gives

$$\frac{\pi(k+\theta+k\theta)\Gamma(1-k)}{\theta^{k+1}(k+1)k} + \frac{1}{(k-1)\theta} + \mathcal{O}\left(\frac{1}{\theta^2}\right).$$

For a given noninteger k (where $\Gamma(1-k)$ is finite), this term goes to zero for large θ with at least $\mathcal{O}\left(\frac{1}{\theta}\right)$. For the case where k is an integer, the expression is simpler $\mathbb{E}\log(1+X) = \psi(k) + \ln(\theta) + \mathcal{O}\left(\frac{1}{\theta}\right)$. Thus we conclude that for large θ, using Lemma 2 instead of Lemma 3 is reasonable. We refer to this as the *high SNR assumption* since $\mathbb{E}X = k\theta$ will correspond to the average SNR in our calculations. As a point of reference, in our simulations the values of k may or may not be integers and typically

$$\mathbb{E}_X \ln(1+X) = \begin{cases} \frac{1}{\Gamma(k)\theta^k} G_{3,1}^{2,3}\left(\begin{matrix} -k, -k+1 \\ -k, -k, 0 \end{matrix} \middle| \frac{1}{\theta} \right) & k \in \mathbb{Z}^+ \\ \psi(k) + \ln(\theta) + \pi \csc(\pi k) \left((-1)^k \left(1 - \frac{\Gamma\left(k, \frac{-1}{\theta}\right)}{\Gamma(k)} \right) - \frac{{}_2F_2\left(1,1;2,2-k;\frac{1}{\theta}\right)}{\Gamma(2)\Gamma(2-k)\Gamma(k)\theta} \right) & k \notin \mathbb{Z}^+ \end{cases} \tag{3}$$

the value is between 1 and 28, while the values for θ may be on the order of 10^2 to 10^5.

B. Sums of Gamma Random Variables

Many of the expressions in this paper involve sums of Gamma random variables with different shape and scale. There are different closed form solutions of the distribution sums of independent Gamma random variables [40], [41] and correlated Gamma random variables [42] (see also the references in the review article [43]). We choose the form in [40] as it gives a distribution that is a sum of scaled gamma distributions.

Theorem 4 (Exact Sum of Gamma Random Variables Distribution): Suppose that $\{Y_i\}_{i=1}^n$ are independent $\Gamma(k_i,\theta_k)$ distributed random variables. Then the probability distribution function of $Y=\sum_i Y_i$ can be expressed as

$$f_Y(y)=C\sum_{i=0}^{\infty}\frac{c_i}{\Gamma(\rho+i)\theta_{min}^{\rho+i}}y^{\rho+i-1}e^{-\frac{y}{\theta_{min}}} \tag{4}$$

where $\theta_{min}:=\min_i\theta_i$, $\rho=\sum_{i=1}^n k_i$, $C=\prod_{i=1}^n\left(\frac{\theta_{min}}{\theta_i}\right)^{k_i}$, and c_i is found by recursion from

$$c_{i+1}=\frac{1}{i+1}\sum_{m=1}^{i+1}m\gamma_m c_{i+1-m} \tag{5}$$

and $\gamma_m=\sum_{i=1}^n k_i m^{-1}\left(1-\frac{\theta_{min}}{\theta_i}\right)^m$.

Proof: See [40]. ∎

For practical implementation, the infinite sum is truncated; see [40] for bounds on the error. Mathematica code for computing the truncated the distribution is found in [42]. The equation in (4) may be used to find an expression for $\mathbb{E}\sum_{i=1}^n X_i$. This is summarized in the following proposition.

Proposition 5: Suppose that $\{X_i\}_{i=1}^n$ are independent $\Gamma(k_i,\theta_k)$ distributed random variables. Then

$$\mathbb{E}\ln\left(\sum_{i=1}^n X_i\right)=\psi(\rho)+\ln(\theta_{min})+C\sum_{m=0}^{\infty}c_m\sum_{i=0}^{m-1}\frac{1}{\rho+i}. \tag{6}$$

Proof: The expectation can be brought into the summation thanks to uniform convergence established in [40]. Then

$$\begin{aligned}\mathbb{E}\ln\left(\sum_{i=1}^n X_i\right)&=\mathbb{E}\ln Y\\&=C\sum_{i=0}^{\infty}\int_{y=0}^{\infty}\frac{c_i}{\Gamma(\rho+i)\theta_{min}^{\rho+i}}\ln y\, y^{\rho+i-1}\\&\qquad\times e^{-\frac{y}{\theta_{min}}}dy \qquad (7)\\&=C\sum_{i=0}^{\infty}c_i\ln(\theta_{min})+C\sum_{i=0}^{\infty}c_i\psi(\rho+i). \qquad (8)\end{aligned}$$

Because (4) is a distribution and sums to one, it follows by integrating that $C\sum_{i=0}^{infty}c_i=1$. Now using the property that $\psi(x+1)=\psi(x)+\frac{1}{x}$, it follows that $\psi(\rho+m)=\psi(\rho)+\sum_{n=0}^{m-1}\left(\frac{1}{\rho+i}\right)$. Substituting into the right hand side of (8), and again using $C\sum_{i=0}^{infty}c_i=1$ gives (4). ∎

In our application of (8) we find that many terms are needed to achieve a reasonable approximation of the summation. Motivated by related work on approximating sums of Chi-squared random variables [44], we suggest a moment matching approximation of (4). This involves approximating the sum with another Gamma random variable with the same first and second order moments, and is rather standard in the statistics community as a way to approximate more complicated distributions [45].

To this end we need the mean and variance of a sum of Gamma random variables, which is summarized in the following lemma.

Lemma 6: Suppose that $\{Y_i\}$ are independent $\Gamma(k_i,\theta_i)$ random variables. The sum $\sum_i Y_i$ has first two moments

$$\mathbb{E}\sum_i Y_i=\sum_i k_i\theta_i \text{ and } \mathbb{E}\left(\sum_i Y_i\right)^2=\sum_i k_i\theta_i^2+\left(\sum_i k_i\theta_i\right)^2 \tag{9}$$

and variance

$$\sum_i \mathrm{var}(Y_i)=\sum_i k_i\theta_i^2. \tag{10}$$

Given a random variable with finite first and second order moments, the second order moment matching Gamma random variable is given in the following Lemma.

Lemma 7 (Gamma 2nd Order Moment Match): Consider a distribution with $\mu=\mathbb{E}X$, $\mu^{(2)}=\mathbb{E}X^2$, and variance $\sigma^2=\mu^{(2)}-\mu^2$. Then the distribution $\Gamma(k,\theta)$ with same first and second order moments has parameters $k=\frac{\mu^2}{\sigma^2}$ and $\theta=\frac{\sigma^2}{\mu}$.

Proof: Setting the first two moments to equality gives $\mu=k\theta$ and $\mu^{(2)}=k\theta^2+k\theta$. Solving for $k=\frac{\mu}{\theta}$ gives $\mu^{(2)}=\mu\theta+\mu^2$, and after simplifying gives $\theta=\frac{(\mu^{(2)}-\mu^2)}{\mu}=\frac{\sigma^2}{\mu}$ and $k=\frac{\mu^2}{\sigma^2}$. ∎

Combining the results in Lemma 6 and Lemma 7, gives the following approximation, which we call the second order Gamma approximation of the sum $\sum_i Y_i$.

Proposition 8 (Sum of Gammas 2nd Order Moment Match): Suppose that $\{Y_i\}$ are independent Gamma distributed random variables with parameters k_i and θ_i. The Gamma distribution $\Gamma(k_y,\theta_y)$ with the same first and second order moments has

$$k_y=\frac{\left(\sum_i k_i\theta_i\right)^2}{\sum_i k_i\theta_i^2}\quad\text{and}\quad\theta_y=\frac{\sum_i k_i\theta_i^2}{\sum_i k_i\theta_i}. \tag{11}$$

Bounds on the maximum error obtained through a moment approximation are known [46] and may be used to estimate the maximum error in the cumulative distribution functions of the Gamma approximation. In Section VII we show that the approximation outperforms the truncated expression in (5) unless a large number of terms are kept, and therefore conclude that the approximation is reasonable. Note that it is exact in some cases, e.g. if all the shape values are identical (in this case $\theta_i=\theta$ then $k_y=\sum_i k_i=\rho$, $\theta_y=\theta=\theta_{min}$ and $c_i=0$).

The moment approximation in Proposition 8 can be used to compute $\mathbb{E}\ln(y)$ using Lemma 2 or $\mathbb{E}\ln(1+y)$ using Lemma 3. The former approach using the first order approximation of

$\psi(x) = \ln(x) + \frac{1}{x} + \mathcal{O}\left(\frac{1}{x^2}\right)$ leads to an especially simple formula

$$\begin{aligned}\psi\left(\frac{\left(\sum_i k_i\theta_i\right)^2}{\sum_i k_i\theta_i^2}\right) &+ \ln\left(\frac{\sum_i k_i\theta_i^2}{\sum_i k_i\theta_i}\right)\\ &\approx \ln\left(\frac{\left(\sum_i k_i\theta_i\right)^2}{\sum_i k_i\theta_i^2}\right) + \frac{\sum_i k_i\theta_i^2}{\left(\sum_i k_i\theta_i\right)^2} + \ln\left(\frac{\sum_i k_i\theta_i^2}{\sum_i k_i\theta_i}\right)\\ &= \ln\left(\sum_i k_i\theta_i\right) + \frac{\sum_i k_i\theta_i^2}{\left(\sum_i k_i\theta_i\right)^2}. \end{aligned} \tag{12}$$

The formula in (12) can be used to derive some intuition about the impact of different channel parameters.

C. Calculation of the Ergodic Rate With Interference

In this paper we are interested in computing average rates for functions of the form $\mathbb{E}\ln\left(1+\frac{X}{\left(\sum_i Y_i+1\right)}\right)$ where X is a Gamma distributed random variable corresponding to the SNR of the desired signal and $\{Y_i\}$ are INRs (interference-to-noise ratios) corresponding to interference signals. In this section we present an approximation that will allow us to compute the ergodic rate under high SNR conditions.

Proposition 9 (High SNR Gamma Rate Approximation): Suppose that X and Y_i are Gamma distributed random variables with parameters (k_x,θ_x) and (k_i,θ_i). Further suppose that $k_x\theta_x \gg 1$ (this is the high SNR assumption). Then (in bits/s/Hz)

$$\begin{aligned}\bar{\mathcal{I}} &= \mathbb{E}\log_2\left(1+\frac{X}{1+\sum_i Y_i}\right)\\ &\approx \mathbb{E}\log_2\left(X+\sum_i Y_i\right) - \mathbb{E}\log_2\left(\sum_i Y_i\right). \end{aligned} \tag{13}$$

Proof: Multiply out the denominators and notice that

$$\begin{aligned}\mathbb{E}\log_2\left(1+\frac{X}{1+\sum_i Y_i}\right) &= \mathbb{E}\log_2\left(1+X+\sum_i Y_i\right)\\ &\quad -\mathbb{E}\log_2\left(1+\sum_i Y_i\right).\end{aligned}$$

Under the high SNR assumption

$$\begin{aligned}\mathbb{E}\log_2\left(1+\frac{X}{1+\sum_i Y_i}\right) &\approx \mathbb{E}\log_2\left(X+\sum_i Y_i\right)\\ &\quad -\mathbb{E}\log_2\left(\sum_i Y_i\right). \end{aligned} \tag{14}$$

■

Calculation of $\bar{\mathcal{I}}$ in Proposition 9 can proceed via finite truncation of the expression in Theorem 5, the Gamma approximation in Proposition 8, or with the digamma approximation in (12).

III. Channel Model

The cellular system with DAS considered in this paper is illustrated in Fig. 1. There is one base station and R RRUs in each cell. The base station and each RRU are equipped with N_t antennas. The subscriber is equipped with $N_r = 1$ receive antennas; extending the results to $N_r > 1$ antennas is an interesting topic for future research. Not all the R RRUs will be active in a given cell, depending on the transmission policy exploited, and furthermore one or more than one user may be selected to receive data.

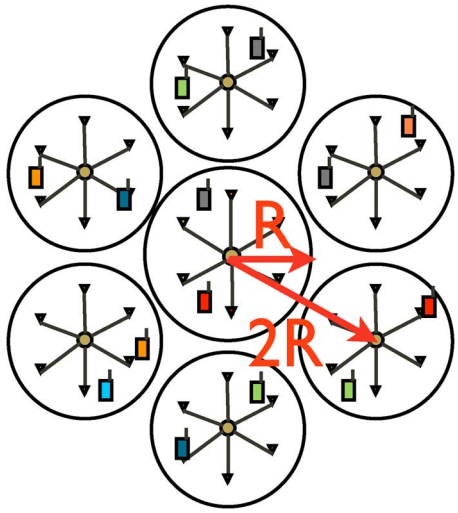

Fig. 1. The distributed antenna system under consideration. Performance is evaluated in a typical cell, accounting for the first tier of interferers. There may be multiple RRUs in a cell with one or more antennas per radio unit.

In this paper we consider a narrowband channel model. The results can be extended to OFDM on a per-subcarrier basis with additional notation. Let us define the $N_r \times N_t$ matrix channel between user u, cell i, and RRU r as $\mathbf{H}_u^{(i,r)}$. The superscript (i,r) is used to indicate the cell $i = 0,1,\ldots,I$ and the remote radio unit $r = 0,1,\ldots,R$ in cell i which is transmitting. The subscript u is used to index the receive users $u = 1,\ldots,U$ who are located in cell i, therefore $\mathbf{H}_u^{(i,r)}$ can be thought of as the in-cell channel, from the transmitters in a cell to the receivers in that cell. Radio unit $r = 0$ corresponds to the base station transmission. Cell $i = 0$ is the "typical" cell where rate calculations will be performed. To compute the interference covariance matrix, the interference channel is also required for users in this cell. Let $\bar{\mathbf{H}}_u^{(i,r)}$ denote the *interference channel* to user $u = 1,2,\ldots,U$ in cell 0 from interfering cell $i = 1,\ldots,I$ and RRU r in interfering cell i. Note that $\bar{\mathbf{H}}_u^{(i,r)}$ denotes the channel to users u in cell $i = 0$ from all the interfering transmitters with $i > 0$, which corresponds to the out-of-cell interference for cell $i = 0$. Because we analyze performance in a typical cell, we do not require notation for the interference channel to users in the interfering cells.

Analysis and simulation of DAS require a channel model that incorporates both small scale and large scale fading effects. In this paper we assume that the entries of $[\mathbf{H}_u^{(i,r)}]_{k,\ell}$ are complex independent $\mathcal{N}(0, L_u^{(i,r)})$ random variables, corresponding to the usual "Rayleigh" assumption. This means that the channel coefficients between antennas are independent. A more realistic model might include spatial correlation between antennas on each RRU; we defer inclusion of spatial correlation to future work. To account for large-scale effects, the variance is chosen

to be $L_u^{(i,r)}$, which denotes the effective received power due to path attenuation from the ith cell and rth RRU to the uth user. For the simulations we use a free-space path loss formula to compute

$$L_u^{(i,r)} = P_r \frac{c^2}{\left(4\pi f_c d_u^{(i,r)}\right)^2} \tag{15}$$

where P_r is the fraction of power allocated to RRU r and $d_u^{(i,r)}$ is the distance between user u in cell i and RRU r in cell i. A more sophisticated distance-dependent received power formula could be used; free-space is just used for simplicity in the simulations. Sectored antennas, which can improve performance in certain configurations [47], can be included through additional direction-dependent gain terms in (15). We similarly assume the interference channel $\bar{\mathbf{H}}_u^{(i,r)}$ is Rayleigh and define the interference path loss $\bar{L}_u^{(i,r)}$ computed from the distance to the interferer $\bar{d}_u^{(i,r)}$. The sum transmit power is assumed to be fixed in each cell, i.e. $\sum_r P_r = P_t$. Spatial power allocation is not considered, nor is power control to combat interference. Both are potentially important techniques but are topics of future work. Log-normal shadowing is not considered in the analysis since our metric of performance will be area spectral efficiency, which is computed by averaging over all locations in the cell. The effects of shadowing can be including by incorporating more sophisticated ray tracing with obstructions in the simulations. In the analysis, shadow fading could be included using a Gamma moment based approximation including small-scale fading and log-normal shadowing [48]; this addition is beyond the scope of this work.

For the purposes of rate calculations, it will be assumed that the in-cell channel state information $\{\mathbf{H}_u^{(i,r)}\}$ is known in each cell, as well as the interference covariance matrix which is determined by the multiuser transmission strategy and is a function of the out-of-cell interference channels. All the cells are assumed to employ the same multiuser transmission strategy at a given time and there is no other coordination between cells. No opportunistic scheduling is considered at present since it complicates the distribution and therefore the ergodic rate calculations. RRU selection decisions are based on in-cell average received signal power.

IV. Multiuser MIMO in a Conventional System

In this section we review the signal model for multiuser MIMO with zero forcing beamforming in non-DAS. We calculate the ergodic rate as a function of user location and develop a Gamma approximation of the rate. The results in this section will be used as a baseline for comparison with our proposed multiuser MIMO DAS approaches.

A. Signal Model

Consider zero forcing multiuser MIMO transmit beamforming from prior work [49], [50] where the beamforming vectors are computed based only on the in-cell channel state information. Without DAS, only RRU $r = 0$ is active, $P_0 = P_t$, and $U \leq N_t$. Let the combined multiuser channel matrix in cell i be defined as

$$\mathbf{H}^{(i,0)} = \left[\mathbf{H}_1^{(i,0)*}, \mathbf{H}_2^{(i,0)*}, \cdots, \mathbf{H}_U^{(i,0)*}\right]^*. \tag{16}$$

The zero forcing precoding matrix $\mathbf{F}^{(i)}$ is derived from the pseudo-inverse of $\mathbf{H}^{(i,0)}$ followed by normalizing the columns. As is customary in the literature, $\mathbf{H}^{(i,0)}$ is assumed to be full rank, which is reasonable if there is enough scattering in the propagation environment. Let $\mathbf{f}_u^{(i,0)}$ denote the u^{th} column of $\mathbf{F}^{(i)}$, which is the beamformer for sending data to user u. Under these assumptions, the received signal at user u in cell 0 is

$$y_u = \mathbf{H}_u^{(0,0)}\mathbf{f}_u^{(0,0)}x_u^{(0)} + \sum_{i=1}^{I} \bar{\mathbf{H}}_i^{(i,0)}\mathbf{F}^{(i)}\mathbf{x}^{(i)} + v_u$$

where v_u is additive white Gaussian noise with distribution $\mathcal{N}(0,\sigma^2)$ and $x_u^{(i)}$ denotes the symbol intended for user u sent from cell i. Zero-forcing perfectly eliminates signal contributions from other in-cell users; therefore in-cell interference disappears from y_u.

B. Rate Calculations

To compute the rate for a given user, we assume Gaussian signaling and treat interference as noise. The ergodic rate for user u is given by

$$\mathcal{I}_u^{MU-MIMO} = \mathbb{E}_{\mathbf{H}} \log\left(1 + \frac{\frac{1}{U\sigma^2}\left\|\mathbf{H}_u^{(0,0)}\mathbf{f}_u^{(0,0)}\right\|^2}{\frac{1}{U\sigma^2}\sum_{i=1}^{I}\bar{\mathbf{H}}_u^{(i,0)}\bar{\mathbf{F}}^{(i)}\bar{\mathbf{F}}^{(i)*}\bar{\mathbf{H}}_u^{(i,0)*} + 1}\right) \tag{17}$$

where $\bar{\mathbf{F}}^{(i)}$ contain the beamformers for the i-th cell. Note that this rate expression is averaged over all channel states and is a function of the user and interference transmitting locations through $L_u^{(i,r)}$ and $\bar{L}_u^{(i,r)}$, though this is not explicitly indicated.

The SINR expression in (17) assumes that zero-forcing is performed with perfect channel state information; therefore the in-cell interference is completely canceled. Imperfect channel state information due to delay or limited feedback, however, will result in nonzero in-cell interference. Further there will be some loss in the signal power. The effects of imperfect channel state information could be included by modifying the signal power and interference terms along the lines of the analysis in [36]. Including imperfect channel state information is a topic of future research.

Exact calculations of (17) are available in special cases for one and two interferers (see, e.g., [51]); general expressions do not seem to be available. For efficient computation with many interferers, and to derive intuition, we approximate (17) using Proposition 9. Comparing (17) to (13), we need to determine k_x, θ_x and k_y, θ_i. Under the Rayleigh channel assumption, $\left(\frac{1}{U\sigma^2}\right)\left\|\mathbf{H}_u^{(0,0)}\mathbf{f}_u^{(0,0)}\right\|^2$ is $\Gamma(k_x,\theta_x)$ with $k_x = N_t - U + 1$ and $\theta_x = \frac{L_u^{(0,0)}}{U\sigma^2}$. This provides the exact form of the Gamma distribution for the signal term.

Computing the distribution of the interference terms in (17) is more complex. Because the interference channel is independent of the channel used to compute $\mathbf{F}^{(i)}$, each term in (17) is a weighted sum of correlated Gamma random variables. The correlation results from the fact that the interfering precoding vectors are nonunitary in the zero-forcing solution; therefore the Gaussian random vector $\mathbf{F}^{(i)*}\bar{\mathbf{H}}_u^{(i,0)*}$ is not spatially white. To avoid this problem, we: (i) assume that the precoding matrices have unit norm orthogonal columns therefore we neglect the correlation; and (ii) use a Gamma approximation through Lemma 7 on the resulting norm. Neglecting the spatial correlation, including the scaling factor $\frac{1}{U\sigma^2}$ each term in (17) is then Gamma distributed with $\Gamma(k_i, \theta_i)$ where $k_i = U$ and $\theta_i = \frac{\bar{L}_u^{(i,0)}}{U\sigma^2}$.

Equipped with the Gamma description of the signal and interference terms, the sum rate can be computed using one of the approaches described in Section II. Because we find the moment matching approach in Lemma 8 gives reasonable performance, we write out the parameters for the calculation according to Proposition 9 here. The sum interference term is approximated as $\Gamma(k_y, \theta_y)$ with parameters

$$k_y = \frac{\left(U\sum_i \bar{L}_u^{(i,0)}\right)^2}{U\sum_i \bar{L}_u^{(i,0)2}} = \frac{U\left(\sum_i \bar{L}_u^{(i,0)}\right)^2}{\sum_i \bar{L}_u^{(i,0)2}} \tag{18}$$

and

$$\theta_y = \frac{1}{U\sigma^2}\frac{\sum_i \bar{L}_u^{(i,0)2}}{\sum_i \bar{L}_u^{(i,0)}}. \tag{19}$$

We approximate the signal plus interference term using

$$k_{xy} = \frac{\left((N_t - U + 1)L_u^{(0,0)}\frac{1}{U\sigma^2} + U\frac{1}{U\sigma^2}\sum_i \bar{L}_u^{(i,0)}\right)^2}{(N_t - U + 1)\left(L_u^{(0,0)}\frac{1}{U\sigma^2}\right)^2 + U\left(\frac{1}{U\sigma^2}\right)^2\sum_i \bar{L}_u^{(i,0)2}} \tag{20}$$

$$= \frac{\left((N_t - U + 1)L_u^{(0,0)} + U\sum_i \bar{L}_u^{(i,0)}\right)^2}{(N_t - U + 1)L_u^{(0,0)2} + U\sum_i \bar{L}_u^{(i,0)2}} \tag{21}$$

and

$$\theta_{xy} = \frac{1}{U\sigma^2}\frac{(N_t - U + 1)L_u^{(0,0)2} + U\sum_i \bar{L}_u^{(i,0)2}}{(N_t - U + 1)L_u^{(0,0)} + U\sum_i \bar{L}_u^{(i,0)}}. \tag{22}$$

The resulting k_x, θ_x, k_{xy}, and θ_{xy} are substituted into (14).

To derive some intuition, we insert this approximation into (12) in (14)

$$\mathcal{I}_u^{MU\text{-}MIMO} \approx \log_2(k_{xy}\theta_{xy}) + \frac{\log_2 e}{k_{xy}} - \log_2(k_y\theta_y) - \frac{\log_2 e}{k_y}$$
$$= \log_2\left(\frac{k_{xy}\theta_{xy}}{k_y\theta_y}\right) + \frac{\log_2 e}{k_{xy}} - \frac{\log_2 e}{k_y}. \tag{23}$$

Looking at the expressions in (18)–(22), in (23) it should be clear that the σ^2 term cancels completely; therefore there is no dependence on the noise power. This makes sense because the high SNR assumption implies that the system is interference, not noise-limited. The first term in (23) is essentially the log of the ratio of the signal plus interference power to the interference power. It is always positive. When the interference power is much lower than the signal power, this term is large; when the interference power is on the order of the signal power this term is small. Also notice that the entire expression is scale invariant. With a distant dependent path-loss model, all the loss factors would be scaled by the same amount and this would cancel in the first term and in k_{xy} and k_y, therefore the capacity is invariant to the cell size.

V. Simplified Multiuser MIMO for DAS

Blanket transmission is a common single user DAS strategy (see e.g. [8]). In this section we propose simplified multiuser MIMO, which is a blanket (or multicast) extension of multiuser MIMO where the base station and all the RRUs share the same beamforming vectors and send the same data. This requires that the RRUs and base station all have the same number of antennas and the maximum number of users is less than or equal to N_t with linear beamforming. The proposed approach is motivated by practical constraints, namely situations when it is not possible to send separate training signals from all RRUs. First we review the signal model for the proposed transmission strategy. Then we calculate the ergodic rate as a function of user location. In the simulations we will show how the proposed approach, despite its simplicity, outperforms conventional MIMO transmission in most settings considered.

A. Signal Model

Suppose that each RRU has $N_t \geq U$ antennas and *will send the same data using the same beamforming vectors* at each RRU to all users in its own cell with zero forcing beamforming. Let the effective matrix for user u in cell i be denoted

$$\mathbf{H}_u^{(i,-)} = \sum_{r=0}^{R} \mathbf{H}_u^{(i,r)}. \tag{24}$$

The sum is used because the base station and RRUs all transmit the same signal therefore the effective channel is a superposition. We use a similar definition for the interference channel $\bar{\mathbf{H}}_u^{(i,-)}$. Let $\mathbf{F}^{(i)}$ be derived from $\mathbf{H}^{(i,-)}$, composed in a similar fashion as (16). Under these assumptions, the received signal at user u in cell 0 is

$$y_u = \mathbf{H}_u^{(0,-)}\mathbf{f}_u^{(0,0)}x_u^{(0)} + \sum_{i=1}^{I} \bar{\mathbf{H}}_u^{(i,-)}\mathbf{F}^{(i)}\mathbf{x}^{(i)} + v_u. \tag{25}$$

Note that the beamforming vectors are applied to the superimposed channel $\mathbf{H}^{(i,-)}$; there is no additional co-phasing therefore no extra array gain.

B. Rate Calculations

We compute the rate for simplified multiuser MIMO using a similar approach as the baseline multiuser MIMO case in Section IV-B. The ergodic rate for user u is given by

$$\mathcal{I}_u^{MU-MIMO,B} = \mathbb{E}_{\mathbf{H}} \log \left(1 + \frac{\frac{1}{U\sigma^2} \left\| \mathbf{H}_u^{(0,-)} \mathbf{f}_u^{(0,0)} \right\|^2}{\frac{1}{U\sigma^2} \sum_{i=1}^{I} \bar{\mathbf{H}}_u^{(i,-)} \mathbf{F}^{(i)} \mathbf{F}^{(i)*} \bar{\mathbf{H}}_u^{(i,-)*} + 1} \right). \quad (26)$$

We propose to calculate (26) using the Gamma random variable approach similar to the previous section. The main difference is to recognize that $\mathbf{H}_u^{(0,-)}$ has independent identically distributed (i.i.d.) entries with distribution $\mathcal{N}(0, \sum_r L_u^{(0,r)})$ and $\bar{\mathbf{H}}_u^{(i,-)}$ has i.i.d. entries with distribution $\mathcal{N}(0, \sum_r \bar{L}_u^{(0,r)})$. Therefore the signal term is $\Gamma(k_x, \theta_x)$ with $k_x = N_t - U + 1$ and $\theta_x = \frac{\sum_r L_u^{(0,r)}}{U\sigma^2}$ while the interference terms in the denominator of (26) are $\Gamma(k_i, \theta_i)$ where $k_i = U$ and $\theta_i = \frac{\sum_r \bar{L}_u^{(0,r)}}{U\sigma^2}$. For a given sum power constraint, in the simplified approach the power would be split among the different RRUs; therefore there is an averaging effect determined by P_r, the power allocated to RRU r.

VI. Full Multiuser MIMO for DAS

In this section we consider full multiuser MIMO, where a beamforming vector is applied across the super array created from the base station and RRUs. The base station designs a beamforming vector of dimension $N_t(R+1) \times 1$ and therefore the system (versus conventional and simplified transmission) can support up to $N_t(R+1)$ users with linear transmission techniques. The disadvantage is an increase in the training overhead to estimate all the channels. First we review the signal model for the proposed transmission strategy. Then we calculate the ergodic rate as a function of user location, and develop a Gamma approximation of the rate. Because of the structure of the composite channel, several additional approximations are required, leveraging some results on isotropic random vectors.

A. Signal Model

Suppose that the base station and RRUs within a cell act as a distributed MIMO antenna array. The beamforming vector is applied to the entire distributed array [30], similar to multicell MIMO (see e.g. [35]). Let the combined multiuser channel matrix be denoted

$$\mathbf{H}^{(0)} = \begin{bmatrix} \mathbf{H}_1^{(0,0)} & \mathbf{H}_1^{(0,1)} & \cdots & \mathbf{H}_1^{(0,R)} \\ \mathbf{H}_2^{(0,0)} & \mathbf{H}_2^{(0,1)} & \cdots & \mathbf{H}_2^{(0,R)} \\ \vdots & \vdots & \vdots & \vdots \\ \mathbf{H}_U^{(0,0)} & \mathbf{H}_U^{(0,1)} & \cdots & \mathbf{H}_U^{(0,R)} \end{bmatrix}. \quad (27)$$

Let $\mathbf{H}_u^{(0)}$ denote the $1 \times N_t(R+1)$ matrix corresponding to user u in $\mathbf{H}^{(0)}$. The zero forcing precoding matrix $\mathbf{F}^{(0)}$ is derived from the pseudo-inverse of $\mathbf{H}^{(0)}$ then normalizing the columns. The multiuser precoders for users in other cells are similarly defined. Under these assumptions, the received signal at user u in cell 0 is

$$y_u = \mathbf{H}_u^{(0)} \mathbf{f}_u^{(0,0)} x_u^{(0)} + \sum_{i=1}^{I} \bar{\mathbf{H}}_u^{(i)} \mathbf{F}^{(i)} \mathbf{x}^{(i)} + v_u.$$

Note that in the simplified multiuser MIMO scenario, we enforce a per-RRU power constraint. Algorithmically, this could be achieved here as well using results from [35], [52]; however, this complicates the analysis. Thus for the MIMO full transmission case, we enforce a sum power constraint. In the related base station cooperation setting, enforcing a per-base station power constraint, e.g. [52], resulted in only a 15% reduction in sum rate performance.

B. Rate Calculations

We can compute the rate with the full multiuser MIMO strategy using a similar approach as the baseline multiuser MIMO case in Section IV-B based on Gamma random variables. The ergodic rate for user u is given by

$$\mathcal{I}_u^{MU-MIMO,DAS} = \mathbb{E}_{\mathbf{H}} \log \left(1 + \frac{\frac{1}{U\sigma^2} \left\| \mathbf{H}_u^{(0)} \mathbf{f}_u^{(0,0)} \right\|^2}{\frac{1}{U\sigma^2} \sum_{i=1}^{I} \bar{\mathbf{H}}_u^{(i)} \mathbf{F}^{(i)} \mathbf{F}^{(i)*} \bar{\mathbf{H}}_u^{(i)*} + 1} \right). \quad (28)$$

Despite the similarity of (28) and (17), approximating the signal and interference terms is complicated due to the block structure in (27). We present calculations that, in simulations, will provide a good approximation within about 10% of the true sum rate.

a) *Signal Term*: This is not straightforward because in Sections IV, V the entries of $\mathbf{H}_u^{(0,0)}$ and $\mathbf{H}_u^{(0,-)}$ are independent identically distributed (i.i.d.) since they have the same variance. In this setup, $\mathbf{H}_u^{(0)}$ has Gaussian entries but with *different* variances, therefore the entries are no longer identically distributed. Thus we cannot apply prior work that exploited properties of i.i.d. Gaussian matrices [51]. If the moments of the signal term were known in this general case, they could be used to compute the moment matched Gamma approximation. Since we are not aware of those results, we suggest the following approximation. To find the shape k_x, we neglect the block structure of $\mathbf{H}_u^{(0)}$ and take $k_x = (R+1)N_t - U + 1$ as predicted from Section IV. This is a good approximation when the path loss to each RRU is similar; otherwise it overpredicts the degrees of freedom. With k_x fixed, we now solve for the scale term by matching the mean in the case that $U = 1$. In this situation, there is no zero-forcing and $\left\| \mathbf{H}_u^{(0)} \mathbf{f}_u^{(0,0)} \right\|^2 = \mathbf{H}_u^{(0)} \mathbf{H}_u^{(0)*}$. Given k_x, we compute $k_x \theta_x = \frac{\mathbb{E}\mathbf{H}_u^{(0)} \mathbf{H}_u^{(0)*}}{U\sigma^2}$ and choose

$$\theta_x = \frac{\mathbb{E}\mathbf{H}_u^{(0)} \mathbf{H}_u^{(0)*}}{(R+1)N_t \sigma^2 U}. \quad (29)$$

We find in simulation that the fit is quite good.

b) *Interference Term*: Now we focus on the interference terms in the denominator of (28). We exploit the independence of the interfering beamforming vectors from the interference channel, and assume the beamforming

vectors in $\mathbf{F}^{(i)}$ are independent isotropic random vectors. To perform these calculations, we use the following facts about expectations with isotropic random vectors.

Lemma 10: Suppose that $\mathbf{v}$ is an $N \times 1$ isotropic random vector and $\mathbf{h}$ is a constant vector. Then

$$\mu_{|\mathbf{h}} := \mathbb{E}_{\mathbf{v}}|\mathbf{v}^*\mathbf{h}|^2 = \frac{\mathbf{h}^*\mathbf{h}}{N}$$

and

$$\mathrm{var}_{|\mathbf{h}}|\mathbf{v}^*\mathbf{h}|^2 = \frac{(N-1)}{(N+1)}\mu_{|\mathbf{h}}^2.$$

Now to remove the conditioning on $\mathbf{h}$ we take the expectation of the conditional results in Lemma 10 for the case where $\mathbf{h}$ is circularly symmetric complex Gaussian with zero mean and potentially different variances per entry.

Proposition 11: Suppose that $\mathbf{h}$ is a $N \times 1$ circularly symmetric complex Gaussian random vector with zero mean and variance σ_n^2 for the n^{th} component and that $\mathbf{v}$ is an isotropic random vector. Then

$$\mu := \mathbb{E}_{\mathbf{v},\mathbf{h}}|\mathbf{v}^*\mathbf{h}|^2 = \frac{1}{N}\sum_n \sigma_n^2$$

and

$$\sigma_v^2 := \mathrm{var}|\mathbf{v}^*\mathbf{h}|^2 = \frac{2(N-1)}{N^2(N+1)}\left(\sum_n \sigma_n^4 + \sum_{n=1}^{N}\sum_{k\neq n}\sigma_n^2\sigma_k^2\right).$$

Proof: Let us denote the k-th entry of $\mathbf{h}$ as h_k. The calculation of μ follows from direction computation: $\frac{\mathbb{E}\sum_{n=1}^{N}|h_n|^2}{N} = \frac{\sum_{n=1}^{N}\sigma_n^2}{N}$ since $\mathbf{h}$ is zero mean. The calculation for σ_v^2 follows from somewhat more tedious calculations. We compute $\mathbb{E}\mu_{|\mathbf{h}}^2 = \sum_{n=1}^{N}\mathbb{E}|h_n|^2 + \sum_{n=1}^{N}\sum_{k\neq n}\mathbb{E}|h_n|^2|h_k|^2 = 2\sum_{n=1}^{N}\sigma_n^4 + 2\sum_{n=1}^{N}\sum_{k\neq n}\sigma_k^2\sigma_n^2$ using Isserlis' Gaussian moment theorem. ∎

Now we compute the Gamma approximation of $\frac{\bar{\mathbf{H}}_u^{(i)}\mathbf{F}^{(i)}\mathbf{F}^{(i)*}\bar{\mathbf{H}}_u^{(i)*}}{U\sigma^2}$ denoted $\Gamma(k_i,\theta_i)$. Assuming that the columns of $\mathbf{F}^{(i)}$ are isotropic random vectors, then $\bar{\mathbf{H}}_u^{(i)}\mathbf{F}^{(i)}\mathbf{F}^{(i)*}\bar{\mathbf{H}}_u^{(i)*}$ is equal in distribution to $\sum_{w=1}^{U}\left\|\bar{\mathbf{H}}_u^{(i)}\mathbf{v}_w\right\|^2$ where $\{\mathbf{v}_w\}$ are independent isotropic random vectors. From Proposition 11, the mean and variance of $\left\|\bar{\mathbf{H}}_u^{(i)}\mathbf{v}_v\right\|^2$ are given by μ and σ_v^2, with $\sigma_n^2 = \frac{\bar{L}_u^{(i,n)}}{U\sigma^2}$. Now applying Lemma 7 and Proposition 8, it follows that $k_i = \frac{U\mu^2}{\sigma_v^2}$ and $\theta_u^{(i)} = \frac{\sigma_v^2}{\mu}$. The resulting expressions can be employed in Proposition 9 using any of the proposed methods for computing the expectation.

VII. Simulations

In this section we present and discuss several Monte Carlo simulation results of the proposed multiuser MIMO DAS. First, we describe the simulation methodology, where the performance is evaluated inside a single cell surrounded by one tier of interferers. Second, we verify the performance of the approximation by examining the rate as a function of distance from the base station and area spectral efficiency. Then we study the rate as a function of the number of users and the effects of radio unit subset selection. Finally, we give some guidance on the impact of the number of RRUs on the overall system performance.

A. Simulation Methodology

The simulation scenario is illustrated in Fig. 1. All cells are circular with radius R_c. The RRUs are uniformly spaced on a ring of distance $\frac{2R_c}{3}$ away from the base station. Unless otherwise mentioned, there are $R = 6$ RRUs. The $I = 6$ interfering base stations are uniformly spaced on a ring of distance $2R_c$ away from the typical base station. Performance in the typical base station $(I = 0)$ is evaluated as a function of distance R_0.

A typical simulation works as follows. For distance R_0 from the base station, a user position on this ring is randomly generated. For $U > 1$ the other users are chosen with uniform location in the cell. These user locations determine $L_u^{(i,a)}$ and $\bar{L}_u^{(i,a)}$ computed assuming 1 W total transmit power and a carrier frequency of $f_c = 2\,\mathrm{GHz}$ using (15). The noise power is computed assuming a temperature of 290 K and a bandwidth of 5 MHz.

The mutual information is therefore computed for the typical user as a function of the distance R_0 from the base station by generating several random locations on the ring of radius R_0 and averaging over various other user locations. The mutual informations in (17), (26), or (28) are calculated using Monte Carlo simulation or one of the proposed approximations, for a given realization of user locations. When Monte Carlo simulation is used to estimate the expectation, 100 different small scale fading matrices $\mathbf{H}_u^{(i,a)}$ and $\bar{\mathbf{H}}_u^{(i,a)}$ are generated and performance is computed for each realization, repeating this process for 120 different locations, for each radius. When different closed form solutions are used to calculate the high SNR rate approximation in Proposition 9, 3,000 user locations are averaged to estimate the mutual information at radius R_0.

To provide a holistic metric of performance we employ the area spectral efficiency (ASE) [37] computed using a discrete approximation as

$$ASE = \left(\pi R_c^2\right)^{-1} U \sum_k \mathcal{I}(R_k)\left(\pi R_k^2 - \pi R_{k-1}^2\right)$$

where R is the cell radius, $\mathcal{I}(R_k)$ is the rate of the user at radius R_k and the last term is the area of the rink between radius R_{k-1} and R_k. For multiple user MIMO communication, we compute the sum ASE, where the ASE for the typical user is multiplied by U, since all users should see typical rate behavior in the cell.

B. Justification of High SNR and Moment Matching Approximations

Before presenting simulation results for DAS, we provide some calculations that justify various different approximations employed in this paper. To address the high SNR assumption, in Fig. 2 we plot the percent error $\frac{(\mathbb{E}\ln(1+X)-\mathbb{E}\ln(X))}{\mathbb{E}\ln(1+X)}$ computed using (3) and (1) for X distributed as $\Gamma(k,\theta)$ as a function of θ for different $k = 1, 2, \ldots, 10$. For values of the scale factor greater than 50, the error is less than 2%. The error is lower for larger values of k and for larger values of θ. In the DAS simulations in this paper, values of k range from 1 to 28 and values of θ are more than 500. Thus we believe the error is small enough

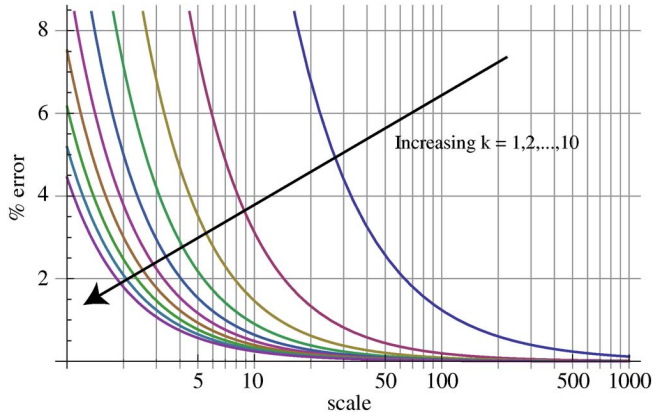

Fig. 2. Percent error in the high SNR approximation as a function of scale θ for different values of $k = 1, 2, \ldots, 10$. For large values of θ, the error is very small.

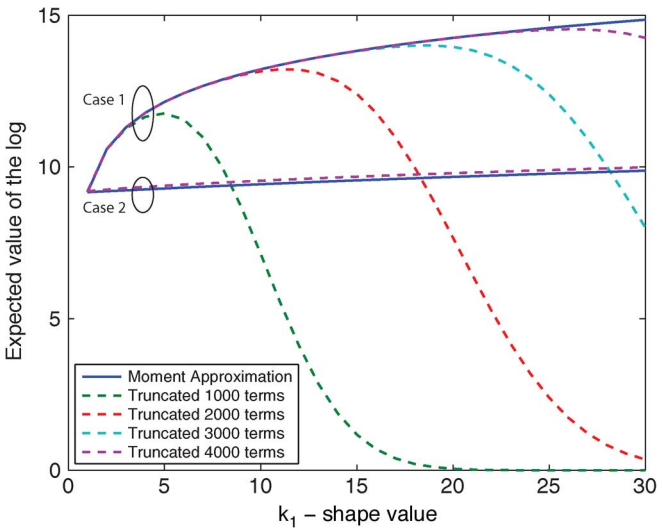

Fig. 3. Percent error in the high SNR approximation as a function of scale θ for different values of $k = 1, 2, \ldots, 10$. For large values of θ, the error is very small.

to justify using (3) to calculate the mutual information instead of the exact expression.

We proposed two different approaches for dealing with the sum of Gamma random variables: the exact expression in Theorem 4 or the moment matching approximation in Proposition 8. In practical calculations, the exact expression will require a finite number of terms in the summation. The exact number of terms depends on the shape factors and the scaling factors. To provide some intuition into the quality of the moment matching approximation, we consider $Y = X_1 + X_2$ where X_1 is $\Gamma(k_1, \theta_1)$ and X_2 is $\Gamma(1, \theta_2)$. We allow k_1 to vary from 1 to 30. We consider two scenarios: (1) $\theta_1 = 10$ and $\theta_2 = 1,000$ and (2) $\theta_1 = 1,000$ and $\theta_2 = 10$ and plot the results in Fig. 3. For case 1, with enough terms, the truncated solution and the moment approximation give essentially the same performance. Note that potentially large numbers of terms are required especially for large values of the shape. For case 2, the truncated and approximate solutions have a small error but the error is constant over most of the range of shape values. We conclude that with enough terms, the truncated and moment approximations give virtually the same performance. This provides the incentives to use the moment matched approximation.

C. Validation of the Rate Approximation

First we present some simulations to give confidence in the application of Proposition 9 using the exact expression for a sum of Gamma random variables in Theorem 4 or the moment matching approximation in Proposition 8. In our simulations, the approximation for the multiuser MIMO baseline and multiuser MIMO simplified cases is quite good, yielding less than one percent error. Due to space limitations, we present curves for the multiuser MIMO full transmission case in Fig. 4. We use 60,000 terms in computing the truncated exact solution. Comparing the simulation and the moment matching approximate solutions, the approximation is worst for a single user, with an error around 5% over most of the radius. The approximation is better for larger numbers of users and at larger radii (where DAS is important). The truncated exact solution lines up perfectly with the moment matched solution, except at the location of the DAS RRUs. At that point, the number of terms in the approximation is not sufficient. With enough terms, the truncated exact solution provides the same performance as our moment based approximation. This means that the error in the approximation in this case is due to our approximations to derive the equivalent Gamma random variables, and not in the approximations of the distribution of the sum. The ASE has negligible errors to five users and a peak error of about 10% for around 14 users. In the case shown, the salient shape features of the curves remain.

Using the truncated exact solution provides performance in between the exact and approximation solutions. While the truncated solution provides a slightly better approximation, the large number of terms in the truncation adds complexity. In our Matlab simulations it takes about 2 hours to compute one curve in the left of Fig. 4, about 200 seconds for the Monte Carlo simulation, and about 2 seconds using the moment based approximation. Consequently, we conclude that (i) our high SNR approximation is reasonable, (ii) our approximation for the performance of MU MIMO with full transmission is reasonable, and (iii) moment matching the sum of Gamma random variable with another Gamma random variable provides a reasonable compromise between complexity and accuracy.

D. Rate as a Function of the Number of Users

Now we present some results on the rate as a function of the number of active users in Fig. 5. In the left plot we illustrate the average per-user rate as a function of distance from the base station. The simplified approach provides worse performance than the conventional approach up to a point, then outperforms the conventional strategy. The peak in the simplified approach occurs at the radius of the RRU deployment $\left(\frac{2}{3R_c}\right)$. From a rate perspective, it seems that switching between conventional and simplified transmission may yield good performance (this also hints that power allocation with simplified transmission may further improve performance). Full transmission provides a modest improvement in per-user rates close to the base station but a more substantial increase further away from the base

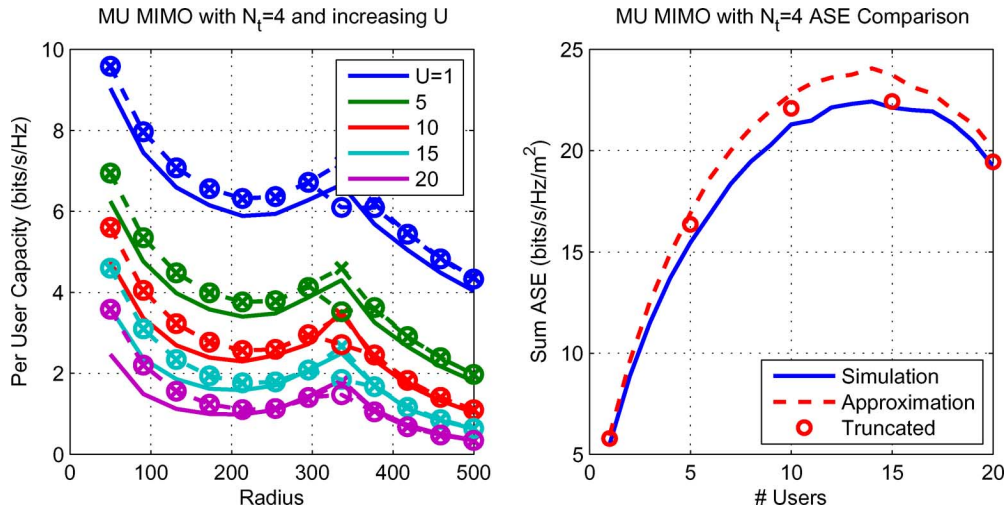

Fig. 4. The rate approximation with multiuser MIMO DAS full transmission. The left plot shows the sum rate as a function of distance from the base station to the cell edge for different values of U. The right plot shows the ASE as a function of U. Solid curves are generated entirely from Monte Carlo simulation, dashed curves are generated using the rate approximation and simulation over user positions. The circle markers indicate the truncated exact solution for the sum terms, while the x markers use the moment matching approximations of the sum terms.

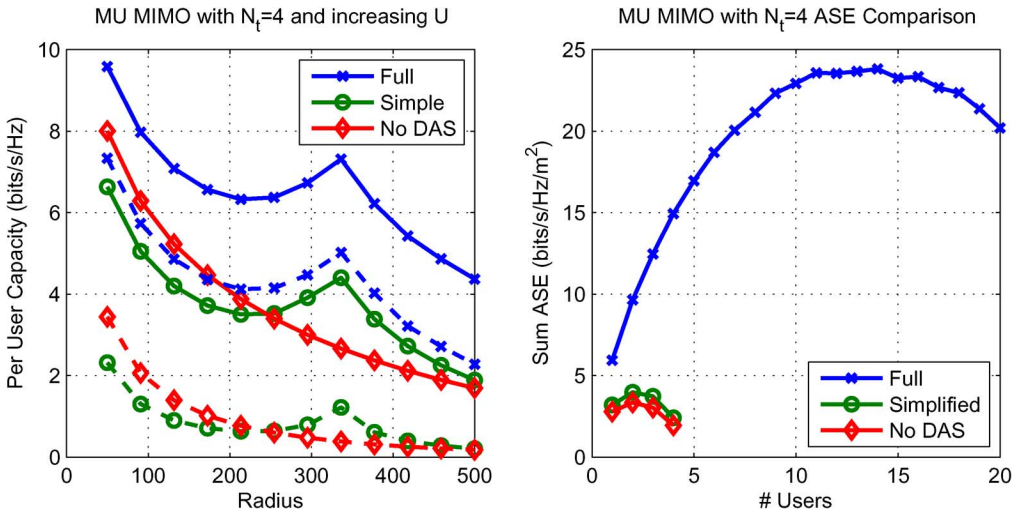

Fig. 5. Comparison of different strategies with $N_t = 4$. The left plot shows the sum rate as a function of distance from the base station to the cell edge for $U = 1$ (solid) and $U = 4$ (dashed). The right plot shows the ASE as a function of U. Only $U = 4$ users are supported for the conventional and the simplified cases. Full transmission supports up to 28 users.

station. Full transmission supports larger numbers of users and, despite the presence of out-of-cell interference, still improves performance at the cell edge.

In the right plot of Fig. 5, we illustrate the ASE as a function of the numbers of users. First, notice that the ASE for the simplified case is somewhat better than the conventional approach, but the ASE of the full transmission is remarkably better. This establishes the significant potential in harnessing of DAS for full multiuser MIMO transmission. Second, notice that there is an optimum number of users for each strategy, corresponding to about half the total number of users that can be supported (14 for the full transmission, and 2 for the simplified and baseline cases). This seems to indicate there is an optimum loading of the system; exceeding the maximum results in reduced ASE and therefore less efficient system operation. For conventional transmission, it has been established that depending on the SNR there is an optimum number of users in terms of ergodic capacity [36]; therefore we expect the loading will be a function of the average SNR, therefore the transmit power, and other system parameters.

E. Varying the Number of RRUs

Now we consider performance for different numbers of RRUs with the same system parameters. From Fig. 6, the performance for all approaches with $R = 0$ is the same as expected. The performance of full transmission grows linearly as the number of RRUs is increased due to the increasing number of users supported simultaneously. The other methods have more moderate growth as the number of RRUs increases. This is interesting because it shows how, at least in the scenario considered, performance continues to grow with increasing numbers of RRUs.

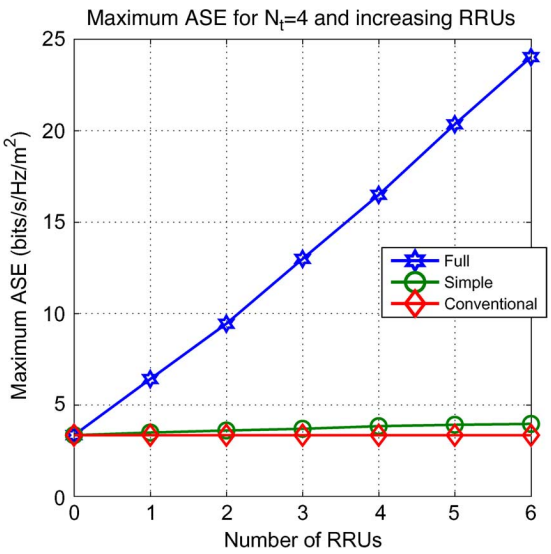

Fig. 6. Comparison of peak ASE for different total numbers of RRUs in the cell. The ASE is simulated for different choices of number of users and the maximum is selected. There is no RRU subset selection in this case.

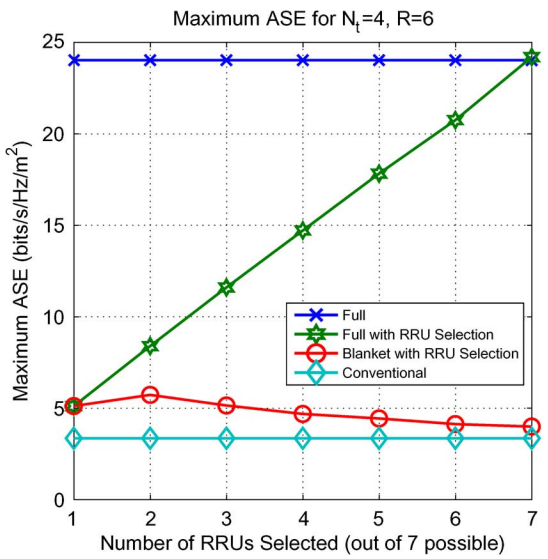

Fig. 7. Illustration of the impact of subset selection on full and simplified transmission on the ASE. The scheduled number of users that provides the maximum ASE was chosen.

Note that because of the total power constraint, the sum interference is not increased as the number of RRUs is increased.

F. Effects of Subset Selection

Now we consider the impact of selecting the best S out of R RRUs, compared with using all available RRUs and with conventional MIMO transmission from a single base station. RRU selection is motivated by results from [8], [21] which show that in single user systems selection diversity is better than blanket transmission, even when channel state information is exploited (equal gain transmission or maximum ratio transmission). To evaluate performance, we propose a simple algorithm that uses only average path loss information within the cell, and is not based on out-of-cell information.

Suppose that the base station selects S out of the $R+1$ radio units for transmission. The case of $S=1$ corresponds to just a single radio unit being active; $S=R+1$ corresponds to all radio units active, which was already considered. Note that for the simplified case $U \leq N_t$, independent of S, while for the full transmission $U \leq N_t S$, for zero forcing beamforming to be effective. We do not consider antenna subset selection at the RRUs. Choosing a subset of RRUs based on statistics is challenging. We cannot use the expressions developed in Sections V, VI because those expressions also include the interference terms, but the interference is a function of the selection strategy in the neighboring cells. We propose to take a greedy approach for RRU selection. Let the set that indexes the radio units be denoted as $\mathcal{R}=\{0,1,\ldots,R\}$ where 0 corresponds to the base station. Randomly permute the indices of the users and let the resulting index set be denoted $\mathcal{U}$. Then starting with the first user in the set $\mathcal{U}$, find the radio unit index in $\mathcal{R}$ that maximizes the average received signal strength. Remove this index from $\mathcal{R}$. Continue for the next user in $\mathcal{U}$. When $S<U$, the first S users in $\mathcal{U}$ receive their preference for closest radio units. If $S>U$ then every user gets a preferred radio unit, and some users may get additional preferred units.

Consider the performance of selection for the simplified and full multiuser MIMO DAS transmission in Fig. 7. First, selecting a subset of RRUs for full MU-MIMO transmission provides worse performance. The reason seems to be that having $S<R$ active RRUs means fewer active users and therefore lower peak ASE. Second, simplified selection has the best performance for two active RRUs. Compared with the right plot in Fig. 5, this peak occurs at $U=2$, corresponding with the ASE peak. Thus for the simplified case, choosing the RRU closest to each user gives the best performance. The potential coverage enhancements from using additional RRUs are overwhelmed by the more spatially uniform interference environment created. Even though simplified transmission gives somewhat poor performance in the other simulation scenarios, in this case there is moderate gain over conventional transmission, which makes the simplified approach with selection still worthwhile. Note that we have not considered practical issues like training and feedback overheads in this comparison, which could change the results if there is an additional penalty to having more RRUs active. This is an interesting extension for future work.

Now we compare Fig. 6, where the number of RRUs is increased, and Fig. 7 where the best RRUs out of a total of $R+1=7$ are selected. The trend for MU-MIMO is similar, with a slight performance improvement for small numbers of RRUs. For the simplified case, performance is better with a peak at two RRUs. From these results we conclude that full MU-MIMO has little to gain from RRU—having more RRUs is best. Alternatively, for simplified MU-MIMO, RRU selection is valuable and can improve performance compared with activating all RRUs.

VIII. Conclusion and Future Work

This paper proposed two different downlink multiuser MIMO DAS transmission strategies. Full multiuser DAS transmission employs all the antennas on the base station and RRUs in a coordinated fashion; blanket multiuser DAS transmission uses

the same beamforming vector at every RRU and the base station. Approximations of the ergodic rate were developed for each of the proposed techniques, using properties of Gamma distributed random variables and approximations of sums of Gamma random variables. The sum rate expressions incorporate explicitly out-of-cell interference, allowing more realistic evaluation of performance in the cellular setting. An algorithm for selecting a subset of RRUs was also proposed.

Simulation results, leveraging the proposed ergodic rate expressions, were used to study the proposed algorithms including interference. In terms of area spectral efficiency, full transmission provided linear growth with increasing number of RRUs while the blanket approach showed only modest performance improvements. Selecting a subset of RRUs for transmission was found to improve the performance of the blanket transmission but to decrease performance of full transmission. In summary, full transmission was found to have the best overall performance for the DAS architecture considered in this paper.

There are several avenues for building on this research. One possibility is to incorporate spatial correlation into the analysis, for example using approximations of sums of Wishart matrices [53]. Another possibility is to incorporate imperfect channel state information, in the form of delay, limited feedback, and feedback overheads. This can be accomplished by leveraging results from [36], for example, to modify the signal power and interference terms. Another possibility is to augment the analysis to allow different transmission configurations in the interfering cells, for example having different numbers of active users. This can be accomplished by modifying the interference parameters and averaging over the different interference states; it is not clear if the analysis can be simplified further. While we developed the analysis for DAS, it can also be applied to other kinds of transmission like femtocells. It is of interesting to study the combined effects of DAS and base station cooperation.

REFERENCES

[1] A. Saleh, A. Rustako, and R. Roman, "Distributed antennas for indoor radio communications," *IEEE Trans. Commun.*, vol. 35, no. 12, pp. 1245–1251, Dec. 1987.

[2] K. J. Kerpez, "A radio access system with distributed antennas," *IEEE Trans. Veh. Technol.*, vol. 45, no. 2, pp. 265–275, May 1996.

[3] H. Yanikomeroglu and E. S. Sousa, "CDMA distributed antenna system for indoor wireless communications," in *Proc. IEEE Int. Conf. Univ. Pers. Commun.*, Oct. 1993, vol. 2, pp. 990–994.

[4] P. Chow, A. Karim, V. Fung, and C. Dietrich, "Performance advantages of distributed antennas in indoor wireless communication systems," in *IEEE Veh. Technol. Conf. (VTC)*, Jun. 1994, vol. 3, pp. 1522–1526.

[5] K. J. Kerpez and S. Ariyavisitakul, "A radio access system with distributed antennas," in *Proc. IEEE Global Telecommun. Conf. (GLOBECOM)*, Nov.–2 Dec. 1994, vol. 3, pp. 1696–1700.

[6] G.-H. Chen, C.-M. Yu, and C.-C. Huang, "A simulation study of a distributed antenna-based CDMA system," in *Proc. IEEE Symp. Pers., Indoor Mobile Radio Commun. (PIMRC)*, Oct. 1996, vol. 2, pp. 517–521.

[7] A. Obaid and H. Yanikomeroglu, "Reverse-link power control in CDMA distributed antenna systems," in *Proc. IEEE Wireless Commun. Netw. Conf. (WCNC)*, 2000, vol. 2, pp. 608–612.

[8] W. Choi and J. G. Andrews, "Downlink performance and capacity of distributed antenna systems in a multicell environment," *IEEE Trans. Wireless Commun.*, vol. 6, no. 1, pp. 69–73, Jan. 2007.

[9] P. Jung, B. Steiner, and B. Stilling, "Exploitation of intracell macrodiversity in mobile radio systems by deployment of remote antennas," in *Proc. IEEE Int. Symp. Spread Spectrum Techn. Appl. (ISSSTA)*, Sep. 1996, vol. 1, pp. 302–307.

[10] M. V. Clark, T. M. I. Willis, L. J. Greenstein, A. J. J. Rustako, V. Erceg, and R. S. Roman, "Distributed versus centralized antenna arrays in broadband wireless networks," in *Proc. IEEE Veh. Technol. Conf. (VTC)*, Rhodes, May 2001, vol. 1, pp. 33–37.

[11] I. Toufik and R. Knopp, "Wideband channel allocation in distributed antenna systems," in *Proc. IEEE Veh. Technol. Conf. (VTC)*, Sep. 2006, pp. 1–5.

[12] R. Pabst, B. H. Walke, D. C. Schultz, P. Herhold, H. Yanikomeroglu, S. Mukherjee, H. Viswanathan, M. Lott, W. Zirwas, M. Dohler, H. Aghvami, D. D. Falconer, and G. P. Fettweis, "Relay-based deployment concepts for wireless and mobile broadband radio," *IEEE Commun. Mag.*, vol. 42, no. 9, pp. 80–89, Sep. 2004.

[13] S. W. Peters, A. Y. Panah, K. T. Truong, and R. W. Heath, Jr., "Relaying architectures for 3GPP LTE-Advanced," *EURASIP J. Adv. Signal Process.*, 2009.

[14] V. Chandrasekhar, J. Andrews, and A. Gatherer, "Femtocell networks: A survey," *IEEE Commun. Mag.*, vol. 46, no. 9, pp. 59–67, Sep. 2008, Toronto, Ont., Canada.

[15] W. Roh, "High performance distributed antenna cellular networks," Ph.D. dissertation, Stanford Univ., Stanford, Apr. 2003.

[16] L. Xiao, L. Dai, H. Zhuang, S. Zhou, and Y. Yao, "Information-theoretic capacity analysis in MIMO distributed antenna systems," in *Proc. IEEE Veh. Technol. Conf. (VTC)*, April 2003, vol. 1, pp. 779–782.

[17] H. Dai, "Distributed versus co-located MIMO systems with correlated fading and shadowing," in *Proc. IEEE Int. Conf. Acoust., Speech Signal Process. (ICASSP)*, May 2006, vol. 4.

[18] H. Dai, H. Zhang, and Q. Zhou, "Some analysis in distributed MIMO systems," *J. Commun.*, vol. 3, no. 9, pp. 43–50, 2007.

[19] W. Roh and A. Paulraj, "Performance of the distributed antenna systems in a multi-cell environment," in *IEEE Veh. Technol. Conf. (VTC)*, Apr. 2003, vol. 1, pp. 587–591.

[20] W. Feng, Y. Li, J. Gan, S. Zhou, J. Wang, and M. Xia, "On the size of antenna cluster in multi-user distributed antenna systems," in *Commun. Netw. China (ChinaCom)*, Hangzhou, Aug. 25–27 2008, pp. 1101–1105.

[21] J. Zhang and J. Andrews, "Distributed antenna systems with randomness," *IEEE Trans. Wireless Commun.*, vol. 7, no. 9, pp. 3636–3646, Sep. 2008.

[22] D. J. Love, R. W. Heath, Jr., V. K. N. Lau, D. Gesbert, B. Rao, and M. Andrews, "An overview of limited feedback in wireless communication systems," *IEEE J. Sel. Areas Commun.*, vol. 26, no. 8, pp. 1341–1365, Oct. 2008.

[23] N. B. Zhang, G. X. Kang, Y. Y. Guo, P. Zhang, and X. Gui, "Adaptive transmitted distributed antenna selection strategy in distributed antenna systems with limited feedback beamforming," *Electron. Lett.*, vol. 45, pp. 1079–1081, Oct. 8, 2009.

[24] E. Zeng, S. Zhu, and Z. Zhong, "On the performance of adaptive limited feedback beamforming in distributed MIMO systems," in *Proc. IEEE Global Telecommun. Conf. (GLOBECOM)*, New Orleans, LA, Nov. 30–Dec. 2008, pp. 1–5, 2008.

[25] D. Gesbert, M. Kountouris, R. W. Heath, Jr, C.-B. Chae, and T. Salzer, "Shifting the MIMO Paradigm," *IEEE Signal Process. Mag.*, vol. 24, no. 5, pp. 36–46, Sep. 2007.

[26] L. Dai, "Distributed antenna system: Performance analysis in multi-user scenario," in *Proc. Conf. Inf. Sci. Syst.*, Mar. 2008, pp. 85–89.

[27] W. Feng, Y. Li, J. Gan, S. Zhou, J. Wang, and M. Xia, "On the deployment of antenna elements in generalized multi-user distributed antenna systems," *Mobile Netw. Appl.*, pp. 1–11, Oct. 2009.

[28] B. Song, R. L. Cruz, and B. D. Rao, "Downlink optimization of indoor wireless networks using multiple antenna systems," in *Proc. INFOCOM*, Mar. 7–11, 2004, vol. 4, pp. 2778–2789.

[29] T. Wu and P. Hosein, "Radio resource management strategies for distributed antenna systems," in *Proc. IEEE Wireless Commun. Netw. Conf. (WCNC)*, Apr. 2010, pp. 1–6.

[30] X. Li, M. Luo, M. Zhao, L. Huang, and Y. Yao, "Downlink performance and capacity of distributed antenna system in multi-user scenario," in *WiCom*, 2009, pp. 1–4.

[31] P. Marsch, S. Khattak, and G. Fettweis, "A framework for determining realistic capacity bounds for distributed antenna systems," in *Proc. Inf. Theory Workshop*, Oct. 2006, pp. 571–575.

[32] P. Marsch and G. Fettweis, "A framework for optimizing the downlink performance of distributed antenna systems under a constrained backhaul," in *Proc. Eur. Wireless Conf.*, 2007.

[33] O. Somekh, O. Simeone, A. Sanderovich, B. M. Zaidel, and S. Shamai, "On the impact of limited-capacity backhaul and inter-users links in cooperative multicell networks," in *Proc. Conf. Inf. Sci. Syst. (CISS)*, March 2008, pp. 776–780.
[34] D. M. Fye, "Design of fiber optic antenna remoting links for cellular radio applications," in *Proc. IEEE Veh. Technol. Conf. (VTC)*, May 1990, pp. 622–625.
[35] J. Zhang, R. Chen, J. G. Andrews, A. Ghosh, and R. W. Heath, Jr., "Networked MIMO with clustered linear precoding," *IEEE Trans. Wireless Commun.*, vol. 8, no. 4, pp. 1910–1921, 2009.
[36] J. Zhang, M. Kountouris, J. G. Andrews, and R. W. Heath, Jr., "Mode switching for the multi-antenna broadcast channel based on delay and channel quantization," *EURASIP J. Adv. Signal Process.*, 2009.
[37] M.-S. Alouini and A. Goldsmith, "Area spectral efficiency of cellular mobile radio systems," *IEEE Trans. Veh. Technol.*, vol. 48, no. 4, pp. 1047–1066, Jul. 1999.
[38] F. Boccardi, H. Huang, and M. Trivellato, "Multiuser eigenmode transmission for MIMO broadcast channels with limited feedback," *IEEE Signal Process. Adv. Wireless Commun.*, pp. 1–5, 17–20, 2007.
[39] R. W. Heath, Jr., T. Wu, Y. H. Kim, and A. C. K. Soong, "Multiuser MIMO in distributed antenna systems," in *Proc. Asil. Conf. Signal, Syst., Comput.*, 2010, pp. 1202–1206.
[40] P. G. Moschopoulos, "The distribution of the sum of independent gamma random variables," *Ann. Inst. Statist. Math. (Part A)*, vol. 37, pp. 541–544, 1985.
[41] S. B. Provost, "On sums of independent gamma random variables," *Statistics*, no. 20, pp. 583–591, 1989.
[42] M.-S. Alouini, A. Abdi, and M. Kaveh, "Sum of gamma variates and performance of wireless communication systems over Nakagami-Fading channels," *IEEE Trans. Veh. Technol.*, vol. 50, no. 6, pp. 1471–1480, Nov. 2001.
[43] S. Nadarajah, "A review of results on sums of random variables," *ACTA Appl. Math.*, vol. 103, no. 2, pp. 131–140, 2008.
[44] A. H. Feiverson and F. C. Delaney, The Distribution and Properties of a Weighted Sum of Chi Squares NASA, Tech. Rep. TN D-4575, 1968.
[45] M. D. Springer, *The Algebra of Random Variables*. New York: Wiley, 1979.
[46] N. I. Akhiezer, *The Classical Moment Problem and Some Related Questions in Analysis*. New York: Oliver Boyd, 1965.
[47] T. Wu, Y. H. Kwon, J. Zhang, and Y. Wang, "Distributed antenna systems with power adjusted beam switching," in *Proc. IEEE Veh. Technol. Conf. (VTC)*, May 2010, pp. 1–5.
[48] S. Al-Ahmadi and H. Yanikomeroglu, "On the approximation of the generalized-K distribution by a gamma distribution for modeling composite fading channels," *IEEE Trans. Wireless Commun.*, vol. 9, no. 2, pp. 706–713, 2010.
[49] Q. H. Spencer, A. L. Swindlehurst, and M. Haardt, "Zero-forcing methods for downlink spatial multiplexing in multiuser MIMO channels," *IEEE Trans. Signal Process.*, vol. 52, no. 2, pp. 461–471, Feb. 2004.
[50] T. Yoo and A. Goldsmith, "On the optimality of multiantenna broadcast scheduling using zero-forcing beamforming," *IEEE J. Sel. Areas Commun.*, vol. 24, no. 3, pp. 528–541, Mar. 2006.
[51] J. Zhang and J. Andrews, "Adaptive spatial intercell interference cancellation in multicell wireless networks," *IEEE J. Sel. Areas Commun.*, vol. 28, no. 9, pp. 1455–1468, Dec. 2010.
[52] H. Dahrouj and W. Yu, "Coordinated beamforming for the multicell multi-antenna wireless system," *IEEE Trans. Wireless Commun.*, vol. 9, no. 5, pp. 1748–1759, May 2010.
[53] D. Nel and C. Van der Merwe, "A solution to the multivariate Behrens-Fisher problem," *Commun. Stat.-Theo. Methods*, vol. 15, no. 12, pp. 3719–3735, 1986.

Robert W. Heath, Jr. (S'96–M'01–SM'06–F'11) received the B.S. and M.S. degrees from the University of Virginia, Charlottesville, in 1996 and 1997, respectively, and the Ph.D. degree from Stanford University, Stanford, CA, in 2002, all in electrical engineering.

From 1998 to 2001, he was a Senior Member of the Technical Staff then a Senior Consultant at Iospan Wireless, Inc., San Jose, CA, where he worked on the design and implementation of the physical and link layers of the first commercial MIMO-OFDM communication system. Since January 2002, he has been with the Department of Electrical and Computer Engineering, The University of Texas at Austin, where he is currently an Associate Professor and Associate Director of the Wireless Networking and Communications Group. He is also President and CEO of MIMO Wireless, Inc. and VP of Innovation at Kuma Signals LLC. His research interests include several aspects of wireless communication and signal processing including limited feedback techniques, multihop networking, multiuser and multicell MIMO, adaptive video transmission, manifold signal processing, and 60-GHz communication techniques.

Dr. Heath has been an Editor for the IEEE TRANSACTIONS ON COMMUNICATION, an Associate Editor for the IEEE TRANSACTIONS ON VEHICULAR TECHNOLOGY, Lead Guest Editor for the IEEE JOURNAL ON SELECTED AREAS IN COMMUNICATIONS Special Issue on Limited Feedback Communication, and Lead Guest Editor for the IEEE JOURNAL ON SELECTED TOPICS IN SIGNAL PROCESSING Special Issue on Heterogenous Networks. He currently serves on the steering committee for the IEEE TRANSACTIONS ON WIRELESS COMMUNICATIONS. He was a member of the Signal Processing for Communications Technical Committee in the IEEE Signal Processing Society. Currently, he is the Chair of the IEEE COMSOC Communications Technical Theory Committee. He was a Technical Co-Chair for the 2007 Fall Vehicular Technology Conference, General Chair of the 2008 Communication Theory Workshop, General Co-Chair, Technical Co-Chair and Co-Organizer of the 2009 IEEE Signal Processing for Wireless Communications Workshop, Local Co-Organizer for the 2009 IEEE CAMSAP Conference, Technical Co-Chair for the 2010 IEEE International Symposium on Information Theory, and is Technical Co-Chair for the 2014 IEEE GLOBECOM Conference. He was a coauthor of Best Student Paper Awards at IEEE VTC 2006 Spring, WPMC 2006, IEEE GLOBECOM 2006, IEEE VTC 2007 Spring, and IEEE RWS 2009, as well as a corecipient of the Grand Prize in the 2008 WinTech WinCool Demo Contest and the EURASIP *Journal on Wireless Communications and Networking* Best Paper Award. He was a 2003 Frontiers in Education New Faculty Fellow. He is the recipient of the David and Doris Lybarger Endowed Faculty Fellowship in Engineering. He is a licensed Amateur Radio Operator and is a registered Professional Engineer in Texas.

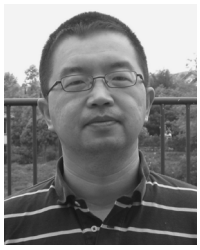

Tao Wu received the B.S. and M.S. degrees in electrical engineering from Shanghai Jiao Tong University, Shanghai, China.

He is currently with Broadcom Corporation with Sunnyvale, CA, as a Principle Engineer on wireless systems design. From 2006 to 2010, he worked for Huawei Technologies (USA), where he has been a Staff Engineer for wireless advanced research and standardizations. From 2000 to 2006, he was with Ericsson Wireless Communication Inc., San Diego, CA, working on CDMA standardizations and radio access networks design. Prior to that, he studied as a Ph.D. candidate with the Department of Electrical and Computer Engineering, University of Utah. His research interests are in wireless communication systems, multiple antenna technologies, radio resource management, and control protocols.

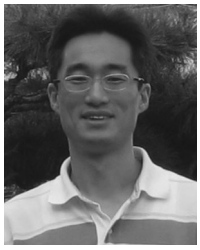

Young Hoon Kwon received the Ph.D. degree from the Department of Electrical Engineering, Korea Advanced Institute of Science and Technology, in 2001.

He is a Senior Staff Engineer with Huawei Technologies, San Diego, CA. He currently works on the solution design and standardization for wireless communication devices, especially for LTE/LTE-A and WLAN devices. Before he joined Huawei Technologies in 2007, he was a Senior Engineer with Samsung Electronics, Suwon, Korea, where he was involved in research and development of CDMA and OFDM-based multiple antenna algorithm design. His research interests span various aspects of physical and MAC layer issues on wireless communication systems, such as MIMO transceiver design, multiuser scheduling algorithm design, and its implementation on wireless terminals.

Anthony C. K. Soong (S'88–M'91–SM'02) received the B.Sc. degree in animal physiology and physics from the University of Calgary, and the B.Sc. degree in electrical engineering, the M.Sc. degree in biomedical physics, and the Ph.D. degree in electrical and computer engineering from the University of Alberta, Alberta, Canada.

He is currently a Principal Engineer for Advance Research and Standards, Huawei Technologies Co. Ltd., in the USA. From 2007 to 2009, he served as the Chair for 3GPP2 TSG-C NTAH (the next generation radio access network technology development group). Currently, he is the Vice Chair for 3GPP2 TSG-C WG3 (the physical layer development group for CDMA 2000). Prior to joining Huawei, he was with the Systems Group for Ericsson Inc. and Qualcomm Inc. His research interests are in statistical signal processing, robust statistics, wireless communications, spread spectrum techniques, multicarrier signaling, multiple antenna techniques, and physiological signal processing. He has published numerous scientific papers and has more than 60 patents granted or pending.

Dr. Soong received the 2005 award of merit for his contribution to 3GPP2 and cdma2000 development. He has served on the Technical Program Committee and has chaired at numerous major conferences in the area of communications engineering. He has acted as Guest Editor for the IEEE *Communications Magazine* and Technical Reviewer for the EURASIP *Journal on Wireless Communications and Networking*, IEEE TRANSACTIONS ON COMMUNICATIONS, IEEE TRANSACTIONS ON WIRELESS COMMUNICATIONS, IEEE TRANSACTIONS ON VEHICULAR TECHNOLOGY, IEEE TRANSACTIONS ON SIGNAL PROCESSING, and IEEE COMMUNICATION LETTERS.